



E-ISSN: 2833-3772 | Volume 4 (2025), Issue 1 | Jan-Feb 2025

The Scientific Journal of Medical Scholar

Publisher and Owner: Real-Publishers Limited (Realpub LLC)

30 N Gould St Ste R, Sheridan, WY 82801, USA

Associate Publisher: The Scientific Society of Educational Services Development [SSESD], Egypt

Website: <https://realpublishers.us/index.php/sjms/index>

**The Scientific Journal of
Medical Scholar**

Available online at Journal Website
<https://realpublishers.us/index.php/sjms/index>
Subject (Microbiology)



Original Article

Construct of *Corallopyronin B* Antibiotic from Heterogeneous Soil Environments in Egypt

Mohammed MS Kassab

Department of Microbiology and Immunology, Faculty of Pharmacy, Cairo University, Egypt.

Article information

Submitted: October, 6th, 2024;

Accepted: November 28th, 2024;

DOI: 10.55675/sjms.v4i1.115

Citation: Kassab MMS. Construct of *Corallopyronin B* Antibiotic from Heterogeneous Soil Environments in Egypt. SJMS 2025 Jan-Feb; 4 (1): 7-22. DOI: 10.55675/sjms.v4i1.115.

ABSTRACT

Background: Antibiotic resistance is an urgent issue everywhere in the globe. It is necessary to look into new sources of antibiotics in order to address this issue.

Aim of the study: Studying the purification of *Corallopyronin B* from various soil conditions in Egypt, as well as the antibacterial effectiveness of *Corallopyronin B* in preclinical animal testing and randomized human clinical trials phases 1/2.

Type of the study: Screening experimental study.

Methodology: Several soil conditions in Egypt were examined to create bacterial isolates that generated the antibiotic chemical *Corallopyronin B*. Using reversed-phase HPLC, *Myxopyronin B* was purified. The test antibiotic's minimum inhibitory concentration (MIC) and in vitro antibacterial activity were ascertained using the paper disc diffusion assay and the broth microdilution technique. Furthermore, in stages 1/2 of randomized clinical trials including human and animal models, pharmacokinetics, adverse drug reactions, and the in vivo antibacterial spectrum were discovered.

Results: The soil bacterial isolate *Coralloccoccus coralloides* DSM 2259, which was grown on Casein yeast peptone (CYP) plate, produced *Corallopyronin B* from its culture supernatant. At MICs more than 100 mcg/ml, the test antibiotic inhibited the growth of many Gram -ve bacteria, including *Escherichia coli*, while also preventing the growth of numerous Gram +ve bacteria, with MICs ranging from 1 to 10 mcg/ml. Eukaryotic cells, on the other hand, including those in humans and fungus, were unharmed. The test antibiotic was shown to have a bactericidal effect by inhibiting bacterial DNA-dependent RNA polymerase (RNLP). In phases 1/2 of randomized human clinical trials, when 600 mg of the dose per 70 kg of body weight was administered SC, the C_{max} was 8.6 mcg/ml at T_{max} 1 hour; T_{1/2} reached 136 min following first order kinetics of elimination. It stopped acting around 6-7 hours after SC was administered. In the preclinical and randomized human clinical trial phases 1/2, less than 6 percent of experimental candidates had uncommon toxicity, which showed up as reduced bile flow. Protein binding with plasma albumin was detected which reached about 83%.

Conclusion: The current work was noteworthy since it involved the production of the bactericidal antibiotic *Corallopyronin B* from *Coralloccoccus coralloides* DSM 2259 that was isolated from several soil environments in Egypt.

Keywords: *Corallopyronin B*; Infection; Antimicrobial; Resistance; Myxobacteria.



This is an open-access article registered under the Creative Commons, ShareAlike 4.0 International license (CC BY-SA 4.0) (<https://creativecommons.org/licenses/by-sa/4.0/legalcode>).

* Corresponding author

Email: mohammed.kassab676@gmail.com

INTRODUCTION

Selective toxicity is a requirement for an antibiotic's medicinal value⁽¹⁾. Compared to human cells, the activity of bacteria must be greatly inhibited⁽²⁾. Since antibiotic resistance is a significant, worldwide difficulty that needs to be addressed, the hunt for new sources of antibiotics is crucial⁽³⁾. Antibacterial medications primarily target four structures: nucleic acids, cell membranes, ribosomes, and cell walls⁽⁴⁾. Due to their lack of a cell wall and the presence of special ribosomes, nucleic acid enzymes, and sterols in their membranes, these medications have no effect on human cells⁽⁵⁾. Antibiotics that are classified as bactericidal are expeditious in killing bacteria⁽⁶⁾. Contrarily, bacteriostatic medications stop the development of microorganisms⁽⁷⁾. The patient's phagocytes eradicate the infection while using bacteriostatic medications⁽⁸⁾. Bacteriocidal medications have to be administered to patients with low neutrophil levels⁽⁹⁾.

Corallopyronins are a class of alpha-pyrone antibiotics⁽¹⁰⁾. A family of heterocyclic chemical compounds is known as pyrones⁽¹¹⁾. They feature a ketone functional group and an unsaturated six-membered ring with one oxygen atom⁽¹²⁾. The terms *4-pyrone* and *2-pyrone* refer to the two isomers⁽¹³⁾. Because *Corallopyronins* do not cross-resistance with any other medicine, they may be able to help solve the developing issue of drug resistance in *TB*⁽¹⁴⁾.

Methicillin-resistant Staphylococcus aureus (MRSA) therapy could potentially be advantageous⁽¹⁵⁾. The cognitive content of the current study was to evaluate the synthesis of a new antibiotic named *Corallopyronin B* under diverse soil conditions in Egypt. In *phase 1/2 randomized clinical trials involving humans*, antibacterial activity was also examined.

PATIENTS AND METHODS

Ethical statement: All relevant institutional, national, and/ or worldwide standards pertaining to the use and care of humans and animals were given priority in the current study. The Ethical Committee for Human and Animal Handling at Cairo University (*ECAHCU*), housed at the Faculty of Pharmacy, Cairo University, Egypt, approved all study procedures involving humans and animals in accordance with the recommendations of the Weatherall Report (approval number *T716/2022*). The number and degree of suffering of the study's human and animal participants were minimized at all costs.

Type of the study: Screening experimental study.

Place and date of the study: The study was consummated at Cairo University's pharmacy faculty in Egypt between *Julie 2022* and *November 2023*.

Source of animal models: The department of pharmacology and toxicology at Cairo University's college of pharmacy provided animal models, which were deemed acceptable.

Inclusion criteria for animal models: Animal models of adult male, obese rabbits weighing approximately 2 kg are available for Inoculation against several bacterial diseases. Before the trial, the rabbits were allowed to acclimatize for one week. At $50\% \pm 5\%$ humidity, a 12-hour light-dark cycle, and a regulated temperature of $25 \pm 2^\circ\text{C}$. Fresh grass was given to the bunnies to eat.

Exclusion criteria for animal models: Young and female rabbits; Non-obese rabbits weighing less than 2 kg.

Collection of 100 soil samples: The samples were randomly selected grassland soils that were taken from various soil settings in Egypt at a depth of 30 cm. Before being processed, samples were kept at 4°C in sterile containers. Each soil sample was weighed out at one gram, and each 250 ml Erlenmeyer flask had 99 ml of sterile distilled water. The flasks were shaken at 400 rpm for five minutes using a gyrator shaker. Following dilutions from 10^{-1} to 10^{-6} in sterile distilled water, the soil suspensions were plated on selective *Casein yeast peptone agar medium* (bought from *Sigma-Aldrich, USA*). 50 cc of nutrient broth liquid at PH 7 was added to 250 ml Erlenmeyer flasks to create the inoculum for the bacterial isolate under investigation. The medium was autoclaved and then infected with a loopful of culture from a nutritional agar slant that had been left overnight. The inoculum was the inoculated flasks, which were shaken for a whole day at 150 rpm.

Instruments

Table (1): List of instruments:

Instrument	Model and manufacturer
Autoclaves	Tomy, japan
Aerobic incubator	Sanyo, Japan
Digital balance	Mettler Toledo, Switzerland
Oven	Binder, Germany
Deep freezer -70°C	Artiko
Refrigerator 5	whirlpool
PH meter electrode	Mettler-toledo, UK
Deep freezer -20°C	whirlpool
Gyrator shaker	Corning gyrator shaker, Japan
190-1100nm Ultraviolet visible spectrophotometer	UV1600PC, China
Light(optical) microscope	Amscope 120X-1200X, China

Materials:

The suppliers of all chemical and biological materials were the Egyptian companies Alnasr Chemical Company and Algomhuria Pharmaceutical Company. Analytical grade chemical reagents were utilized in all cases.

Isolation of *Corallococcus coralloides* DSM 2259 producing Coralopyronin antibiotics:

The selective isolation of species of *Corallococcus coralloides* DSM 2259 from different soil samples was directly achieved using dilution plating. The technique comprised the suppression of competing bacteria exploiting antibiotics such as 10 mcg/ml Vancomycin and/ or 10 mcg/ml Chloramphenicol combined with wet heat treatment of soils and air drying. Fungi were eliminated via supplementing the plating medium with 2 mcg/ml Terbinafine HCl. Swarming of *Corallococcus coralloides* DSM 2259 colonies was controlled with Casein Yeast Peptone (CYP) plates incubated at 30°C and PH 7.2 for 5 days. The constitution of CYP plate included 0.4 % Peptone from Casein, typically digested, 0.3 % CaCl₂.2H₂O, 0.1 % MgSO₄.7H₂O, PH 7.2. The potent bacterial isolate producing Myxopyronin was performed utilizing 16 S rRNA sequencing technique. The predominant bacterial isolate with high antibacterial activity was identified using 16S rRNA sequencing and other biochemical tests. Nucleic acid was extracted from a swab by bead-beating in a buffered solution containing Phenol, Chloroform and Isoamyl alcohol. Variable region of 16S rRNA gene was then amplified from the resulting nucleic acid using PCR. The genomic DNA was extracted from 120 hours cultured cells using a DNA purification kit [PurreLink™ Genomic DNA Mini Kit with Catalog number: K182002 was purchased from Invitrogen, USA] according to the protocol provided by the manufacturer of DNA purification kit. The 16S rRNA gene was amplified by PCR [PCR SuperMix kit was purchased from Invitrogen, USA] using forward [5'-AGAGTTTGATCCTGGCTCAG-3'] and reverse [5'-GGTACCTTGTTACGACTT-3'] primers. PCR amplicons from up to hundreds of samples were then combined and sequenced on a single run. The resulting sequences were matched to a reference database to determine relative bacterial abundances. Polymerase Chain Reaction (PCR) was a powerful method for amplifying particular segments of DNA. PCR used the enzyme Platinum™ Taq DNA polymerase with catalog number 1096601 [purchased from Invitrogen, USA] that directed the synthesis of DNA from deoxynucleotide substrates on a single-stranded DNA template. DNA polymerase added nucleotides to the 3' end of a custom-designed oligonucleotide when it was annealed to a longer template DNA. Thus, if a synthetic

oligonucleotide was annealed to a single-stranded template that contained a region complementary to the oligonucleotide, DNA polymerase could use the oligonucleotide as a primer and elongate its 3' end to generate an extended region of double stranded DNA. **Denaturation was the initial PCR cycle stage** The DNA template was heated to 94° C. This broke down the weak hydrogen bonds that held DNA strands together in a helix, allowing the strands to separate creating single stranded DNA. **Annealing was the second PCR cycle.** The mixture was cooled to anywhere from 50-70° C. This allowed the primers to bind (anneal) to their complementary sequence in the template DNA. **Extension was the final step of PCR cycle.** The reaction was then heated up to 72° C, the optimal temperature for DNA polymerase to act. DNA polymerase extended the primers, adding nucleotides onto the primer in a sequential manner, using the target DNA as a template. With one cycle, a single segment of double-stranded DNA template was amplified into two separate pieces of double-stranded DNA. These two pieces were then available for amplification in the next cycle. As the cycles were repeated, more and more copies were generated and the number of copies of the template was increased exponentially. The amplified PCR product was sequenced using a genetic analyzer 3130XL [purchased from Applied biosystems, USA]. DNA sequence homology search analysis of the predominant bacterial isolate was achieved using Blastn algorithm at NCBI website. Fruiting bodies were examined using a Stereomicroscope(dissecting microscope) MSC-ST45T(purchased from Infetik, China). Wet mounts from crushed fruiting bodies were prepared. The refractility, shape and the size of Myxospores were determined employing phase contrast microscopy. On the other hand the plates were exposed to 360 nm wavelength ultraviolet light to assess the fruiting bodies fluoresced⁽¹⁶⁾.

Identification Myxopyronin B producing bacterial isolates:

Gram stain: It classified bacteria into two categories based on the makeup of their cell walls. The bacterial cells became purple after being treated with a solution of crystal violet and subsequently iodine on a microscope slide. When colored cells were treated with a solvent such as alcohol or acetone, gram-positive organisms kept the stain whereas gram-negative organisms lost the stain and turned colorless. With the addition of the counter-stain safranin, the clear, gram-negative bacteria became pink⁽¹⁷⁾.

Spore shape: This was discovered using the spore staining method. To get rid of any fingerprints, the slide was wiped with alcohol and a Kim-wipe. On the bottom of the slide, a Sharpie was used to create two circles. Each

circle was filled with two tiny droplets of water using an inoculation loop. A very small amount of germs was taken out of the culture tube using an aseptic method. The water droplet on the slide had microorganisms on it. The slide was thoroughly dried by air. Bypassing the slide through the flame three to four times with the smear side up, the slide was heat-fixed. It took a while for the slide to completely cool. A piece of paper towel placed inside the slide's border was used to hide the streaks. A beaker of heating water was situated over the slide. The slide was allowed to steam for three to five minutes; while the paper towel was covered with a malachite green liquid. Removed and thrown away was the discolored paper towel. To get rid of any stray paper towel bits, the slide was gently cleaned with water. The counter-stain was safranin for 1 minute. Before putting the slide on the microscope's stage and seeing it via the oil immersion lens, the slide's bottom was dried⁽¹⁸⁾.

Spore site: During the Gram stain test, the spore location was established⁽¹⁹⁾.

Cell shape: During the Gram stain test, the cell shape was assessed⁽²⁰⁾.

Blood haemolysis: On blood agar media, the test antibiotic capacity to haemolyze the blood was tested⁽²¹⁾.

Motility test: It discriminated between motile bacteria and non-motile bacteria. A sterile needle was used to penetrate the medium to within 1 cm of the tube's bottom to select a well-isolated colony and test for motility. The needle was certainly retained in the same position as it was inserted and removed from the medium. It took 18 hours of incubation at 35°C, or until noticeable growth appeared⁽²²⁾.

Nitrate reduction test: 0.5 ml of nitrate broth was added in a clean test tube, was autoclaved for 15 minutes at 15 lbs pressure and 121°C, and was let to cool to room temperature. The tube was inoculated with a heavy inoculum of fresh bacterial culture and was incubated at 35°C for 2 hours. 2 drops of reagent A and 2 drops of reagent B were added and mixed well. The development of red color within 2 minutes was observed for. If no red color was developed, a small amount of zinc dust was added and observed for the development of the red color within 5 minutes⁽²³⁾.

Methyl red test: In the Methyl Red test, an infected tube of MR broth was used before adding the methyl red PH indicator. The buffers in the medium were overcome by the acids when an organism used the mixed acid fermentation pathway and produced stable acidic end products, resulting in an acidic environment⁽²⁴⁾.

Catalase test: A little inoculum of a specific bacterial strain was introduced to a 3% hydrogen peroxide solution to see if it might produce catalase. It was observed for the rapid emergence of oxygen bubbles⁽²⁵⁾.

Oxidase test: The 1% Kovács oxidase reagent was applied to a tiny piece of filter paper, which was then allowed to air dry. A well-isolated colony was taken from a fresh (18 to 24-hour culture) bacterial plate using a sterile loop, and it was then rubbed onto prepared filter paper. Color alterations were noticed⁽²⁶⁾.

Citrate utilization: Five milliliters of a Simmon Koser's citrate medium were taken after it had been autoclaved at 15 pounds for 15 minutes. To create a clear slant and butt, the test tube containing melted citrate medium was slanted. Using sterilized wire and labeled tubes, the specified samples of microbe were injected on the media's incline. For 24 hours, the tubes were incubated at 37°C. The medium's color shift was watched for⁽²⁷⁾.

Starch hydrolysis: For 48 hours at 37°C, the bacterium plates were injected. After incubation, a dropper was used to saturate the surface of the plates with an iodine solution for 30 seconds. Iodine that was in excess was afterward poured out. The area surrounding the bacterial growth line was looked at⁽²⁸⁾.

Tween 80 hydrolysis: 1% Tween 80 was used to create agar media. The supplied microorganism was added to the Tween 80 agar plates by utilizing an inoculating loop to create a single center streak in the plate. The plates were incubated for 24 hours at 37 °C. HgCl₂ solution was poured over the plates. After a short while, the plates were examined. Positive test result; distinct halo-zone surrounding the injected region showed Tween 80 hydrolysis⁽²⁹⁾.

Growth at 10-45 °C: On nutrient agar media, growth was observed to be possible at 10-45°C⁽³⁰⁾.

Indol test: The test tube containing the microorganism for inoculation received 5 drops of the Kovács reagent directly. Within seconds after introducing the reagent to the media, the reagent layer formed a pink to red color (cherry-red ring), which was a sign of a positive indol test⁽³¹⁾.

Tolerance salinity test: Its capacity to develop on nutrient agar while being responsive to 5% and 7 % NaCl was examined⁽³²⁾.

Voges-Proskauer (VP) test: For the test, Voges-Proskauer broth, a glucose-phosphate broth loaded with microorganisms, was added to alpha-naphthol and

potassium hydroxide. A successful outcome was indicated by a cherry red tint, whereas an unfortunate outcome was indicated by a yellow-brown color⁽³³⁾.

Casein hydrolysis test: For testing the casein hydrolyzing activity of the test antibiotic, a single line streak of the given culture was made in the center of the skim milk agar plate under aseptic conditions and plate was incubated at 37°C in an incubator for 24-48 h⁽³⁴⁾.

Saccharide fermentation tests:

Glucose fermentation test: The fermentation reactions of glucose were investigated using glucose purple broth. Peptone and the PH indicator bromocresol purple made up the purple broth. A 1% concentration of glucose was added. Isolated colonies from a 24-hour pure culture of microorganisms were added to the glucose purple broth as an inoculant. Parallel to the inoculation of the glucose-based medium, a control tube of purple broth base was used. The inoculated medium was incubated aerobically for 3 days at a temperature of 35–37 °C. The medium began to become yellow, which was a sign of a successful outcome. A poor carbohydrate fermentation response was indicated by the lack of yellow color development⁽³⁵⁾.

Fructose fermentation test: A pure culture's inoculum was aseptically transferred to a sterile tube of phenol red fructose broth. The infected tube was incubated for 18–24 hours at 35–37 °C. A color shift from red to yellow, signifying an acidic PH alteration, was a sign of a favorable response⁽³⁶⁾.

Maltose fermentation test: A pure culture inoculum was aseptically transferred to a sterile tube containing phenol red maltose broth. The infected tube was incubated for 18–24 hours at 35–37 °C. A color shift from red to yellow, signifying an acidic PH alteration, was a sign of a favorable response⁽³⁷⁾.

Sucrose fermentation test: A pure culture's inoculum was aseptically transferred to a sterile tube containing phenol red sucrose broth. For 24 hours, the infected tube was incubated at 35–37 °C. A color shift from red to yellow, signifying an acidic PH alteration, was a sign of a favorable response⁽³⁸⁾.

Purification of *Corallopyronin B* antibiotic:

This was achieved through reversed phase chromatography technique. The aeration rate was 0.142 V/ V. min. The stirring rate was 500 rpm. PO₂ was about 90 % of saturation; but decreased to about 20 % after 18 hours). The fermentation was stopped after 40 hours via centrifugation

at 500 rpm in a gyrator shaker. The supernatants were collected; then tested for antimicrobial sensitivity using broth dilution technique to detect MICs and agar paper diffusion discs technique. The test antibiotic was extracted from the 2 liters of culture broth with 2/ 10 volume ethyl acetate. The ethyl acetate was then removed under the reduced pressure at 40°C. Afterwards, the residue was dissolved in 398 ml of methanol-water (90:10) and chromatographed on reversed phase HPLC. Methanol was the mobile phase. The eluent was 70 part methanol: 16 part water: 4 part acetic acid with flow rate 300 ml/ min. Detection of the antibiotic components was achieved exploiting refractive index. The main peak with retention time 5 minutes contained the biological antibiotic activity which was determined via agar diffusion assay using paper discs and *Staphylococcus aureus* as an indicator organism. On the other hand, the main peak was subjected to neutralization via NaHCO₃. *Corallopyronin A* was extracted using 10 % V/ V Methylene chloride. After the evaporation of the solvent, about 87 % of the antibiotic substance purified was *Corallopyronin B*. It was noticed that the retention time of *Corallopyronin B* was 9 minutes. Molecular formula of the purified *Corallopyronin B* was detected through mass spectrometer (Quadrupole mass spectrometer, Advion, USA)⁽³⁹⁾. It was detected also, that 13% of *Corallopyronin mixture extract* were 7% *Corallopyronin A* and 6% *Corallopyronin C*.

Procedure of Broth dilution assay for determination of MICs of *Corallopyronin B*:

A specific broth was added to several microtiter plates during the testing process based on the requirements of the target bacterium. The test microorganisms and antibiotics were then introduced to the plate in varying amounts. After that, the plate was put into a non-CO₂ incubator and left there for sixteen to twenty hours at 37 degrees Celsius. The plate was taken out and examined for bacterial growth after the specified amount of time had passed. Bacterial growth was detected in the cloudiness of the broth. The lowest concentration of antibiotics that prevented bacterial growth, or Minimum Inhibitory Concentration (MIC), was used to describe the outcomes of the broth microdilution method⁽⁴⁰⁾.

Agar diffusion assay with paper discs procedure for the determination of *Corallopyronin B* antimicrobial activity:

The agar diffusion technique (ADM) was used to classify the disc diffusion method (DDM) because the test microorganism-seeded agar media allowed the test antibiotic extract to disperse from its reservoir. A filter paper disc put on an agar surface served as the reservoir

most of the time. After the filter paper disc was incubated, an inhibitory zone formed around the tested extract chemicals that were microbiologically active. The test extract's antibacterial potency was accurately reflected by the inhibition zone's diameter⁽⁴²⁾.

Both broth and selection or enrichment growing media were used to isolate the test microorganisms (Table 2).

Table (2). It demonstrates different isolation media for different pathogenic m.os. utilized in the *Broth microdilution* test and agar diffusion assay using paper discs

Pathogenic m.o	No of strains	Isolation media
<i>Bacillus subtilis</i>	5	Mannitol egg yolk polymixin agar(MEYP)
<i>Bacillus cereus</i>	7	Polymixin egg yolk mannitol bromothymol blue agar(PEMBA)
<i>Staphylococcus aureus</i>	6	Salt mannitol agar(SMA)
<i>Pneumococci</i>	13	Todd Hewitt broth with yeast extract
<i>E. coli</i>	17	Sorbitol- Macconkey agar
<i>Pseudomonas aeruginosa</i>	10	<i>Pseudomonas</i> isolation agar(PSA)
<i>Candida albicans</i>	1	Potato dextrose agar(PDA)
<i>Saccharomyces cerevisiae</i>	5	Sabourad dextrose agar(SDA)
<i>Salmonella typhimurium</i>	4	Bismuth sulfite agar(BSA)
<i>Haemophilus influenza</i>	3	Enriched chocolate agar
<i>Gonococci</i>	4	Thayer martin medium
<i>meningococci</i>	6	Mueller Hinton agar
<i>Serratia Marcescens</i>	4	Caprylate thallous agar medium
<i>Mucor hiemalis</i>	1	Potato dextrose broth
<i>Shigella dysenteriae</i>	8	Hektoen enteric agar
<i>Micrococcus luteus</i>	1	Tryptic soy agar
<i>Proteus mirabilis</i>	1	Blood agar
<i>Chlamydiae pneumoniae</i>	1	<i>Chlamydiae pneumoniae</i> Monkey cell culture
<i>Rickettsiae typhi</i>	1	Chicken embryos culture

Estimation of *Corallopyronin B* effect on bacterial RNA synthesis:

The concentration of RNA isolated with *RNeasy Kits* (purchased from *QIAGEN, USA*) was determined by measuring the absorbance at 260nm in a spectrophotometer. An absorbance of 1 unit at 260 nm corresponds to 40µg of RNA per ml ($A_{260} = 1 = 40 \mu\text{g/ml}$).⁴²

Estimation of *Corallopyronin B* effect on bacterial protein synthesis:

Absorbance was measured at 205 nm to calculate the protein concentration by comparison with a standard curve. A (205) method could be used to quantify total protein in crude lysates and purified or partially purified protein. The UV spectrophotometer was set to read at 205 nm allowing 15 min for the instrument to equilibrate. The absorbance reading was set to zero with a solution of the buffer and all

components except the protein present. The protein solution was placed in the 1 ml cuvette and the absorbance was determined. The dilution and readings of samples were performed in duplicate. The matched cuvettes for samples and controls were utilized during the test procedure. The extinction coefficient of the protein was known, the following equation was used. $\text{Absorbance} = \text{Extinction coefficient} \times \text{concentration of protein} \times \text{path length (1cm)}$ to determine the concentration of the protein⁽⁴³⁾.

Estimation of pharmacodynamic and pharmacokinetic effects of *Corallopyronin B* during experimental animal testing in preclinical clinical trials:

In the present study, the pharmacokinetics and the pharmacodynamics of *Corallopyronin B* were evaluated after dosing in male rabbit animal models weighing about 2kg.

Furthermore, compound concentrations were determined in target compartments, such as lung, kidney and thigh tissue, using *LC-MS/ MS*. Based on the pharmacokinetic results, the pharmacodynamic profile of *Corallopyronin B* was assessed victimizing the standard neutropenic thigh and lung infection models⁽⁴⁴⁾.

Estimation of pharmacodynamic and pharmacokinetic effects of *Corallopyronin B* in randomized human clinical trials phases 1/2:

This study was conducted in 150 human volunteer subjects to show the bioavailability, pharmacokinetics and the pharmacodynamics of the test antibiotic. The study was designed as randomized, single-dose, 2-treatment, 2-period crossover trial with a washout period of 1 week. Blood samples were collected at 0(baseline), 10, 20, and 40 minutes and at 1, 1.5, 2, 3, 4, 6, 9, 12, and 24 hours postdose.

Plasma concentrations of the 4 drugs were measured by using a rapid chromatography-tandem mass spectrometry method. Pharmacokinetic parameters were calculated by using noncompartmental methods. Bioequivalence was determined if the 90 % CIs of the log-transformed test/reference ratios $AUC(0-26)$, $AUC(0-\infty)$, and C_{max} were within the predetermined range of 80% to 125%.

Tolerability was assessed by using clinical parameters and subject reports Pharmacodynamic effects were evaluated through the determination of MICs via agar diffusion assay and broth dilution technique During *randomized human clinical trials phases 1/2* all utilized infectious bacterial cell counts were estimated spectrophotometrically⁽⁴⁵⁾.

Estimation of phototoxicity, mutagenicity and carcinogenicity of the test antibiotic:

The phototoxicity of *Corallopyronin B* was determined via *3T3 neutral red uptake* phototoxicity technique⁽⁴⁶⁾. On the other hand, *mutagenicity* and *carcinogenicity* of the test antibiotic were assessed using *Ames test*⁽⁴⁷⁾.

The determination of toxokinetic and toxodynamic effects:

Up and down method for acute toxicity detection of *Corallopyronin B* was utilized for this purpose⁽⁴⁸⁾.

The determination of maximum bactericidal activity of Corallopyronin B:

A pure culture of a specified microorganism was grown overnight, then diluted in growth-supporting broth (typically *Mueller Hinton Broth*) to a concentration between 1×10^5 and 1×10^6 cfu/ml. A stock dilution of the antimicrobial test substance was made at approximately 100 times the expected MIC. Further 1:1 dilutions were made in test tubes. All dilutions of the test antibiotic were inoculated with equal volumes of the specified microorganism. A positive and negative control tube was included for every test microorganism to demonstrate adequate microbial growth over the course of the incubation period and media sterility, respectively. An aliquot of the positive control was plated and used to establish a baseline concentration of the microorganism used. The tubes were then incubated at the appropriate temperature and duration. Turbidity indicated growth of the microorganism and the MIC was the lowest concentration where no growth was visually observed. To determine the MBC, the dilution representing the MIC and at least two of the more concentrated test product dilutions were plated and enumerated to determine viable CFU/ml. The MBC was the lowest concentration that demonstrated a pre-determined reduction (such as 99.9%) in CFU/ml when compared to the MIC dilution⁽⁴⁹⁾.

Determination of plasma protein binding capacity of Corallopyronin B:

Employing an ultrafiltration technique, the protein binding (PB) extent and changeability of the test antibiotic medicates were settled when given simultaneously to 30 patients inoculated with infectious *pneumococci* inside hospitals in Egypt. Clinical samples used were routinely received by microbiological laboratory inside the faculty of Pharmacy, Cairo University, Egypt. Plasma proteins were likewise plumbed. A protein-free medium was used to determine the nonspecific binding. Plasma samples from 30

patients were enclosed, of which plasma proteins were deliberated for 24 patients.

Determination of liver, kidney and heart function tests after addition of Corallopyronin B:

These functional tests were performed to assess the vitality of *liver*, *kidney* and *heart* during the randomized human clinical trials phases 1/2. On the other hand, Urine, stool analyses were achieved in addition to estimation of *complete blood counts* to all experimental subjects which received graded doses of *Corallopyronin B*.

Formulation of Corallopyronin B (COR B):

A liquid solution (COR B > 30 mg ml⁻¹) comprising *polyethylenglycol-15-hydroxystearate* (35%), *propylene glycol* (15%), and *phosphate buffered saline pH 7.3* (75%), as excipients, was prepared for IV and SC administration. PEG 400(50%) and *phosphate buffered saline pH 7.3* (60%) were added to a liquid formulation that included COR B for human effectuality attempts administered by oral and SC methods. For toxicity tests, a liquid COR B formulation based on PEG 200 that permitted an oral dosage of 1500 mg kg⁻¹ (150 mg ml⁻¹) was created. Each formulation exhibited adequate COR B in-use stability.

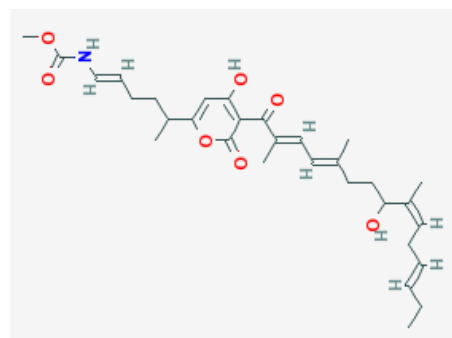


Figure (1). It demonstrates the structure of *Corallopyronin B* extracted from bacterial isolates *Coralloccoccus coralloides* DSM 2259 collected from different soil environments in Egypt. Molecular formula of the purified test antibiotic was noticed to be C₃₁H₄₂NO₇ determined through mass spectrometer.

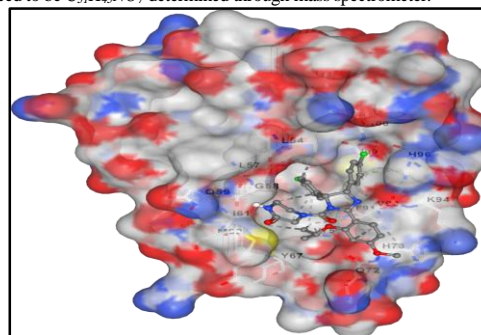


Figure (2). It represents docking of *Corallopyronin B* ligand on Bacterial RNA polymerase. *Corallopyronin B* showed high affinity and inhibitory effect towards the switch region of RNA Polymerase. Molecular mass of *Corallopyronin B* was observed to be nearly 540 Da. ΔG was found to be roughly 15 J/mol; nevertheless it was discovered that the test antibiotic's Kd near the switch area was roughly -720 nM.

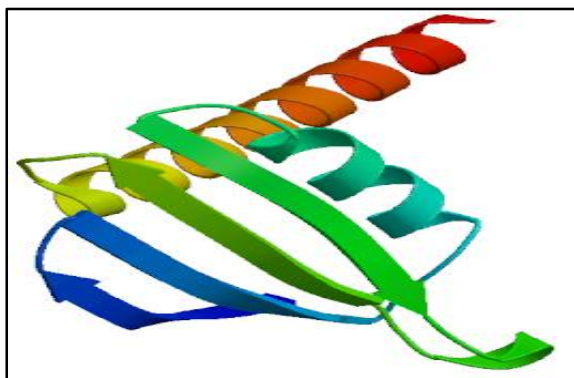


Figure (3). It demonstrates 3D structure of bacterial prokaryotic RNA polymerase comprising the switch binding site to which *Corallopyronin B* Ligand strongly bound inhibiting bacterial RNA polymerase activity selectively leading to the inhibition of mRNA transcription and subsequently the mortality of the microbe. The secondary structure of RNA polymerase enzyme consisted of spiral alpha and beta sheets. Its molecular mass was approximately 198 amino-acids.

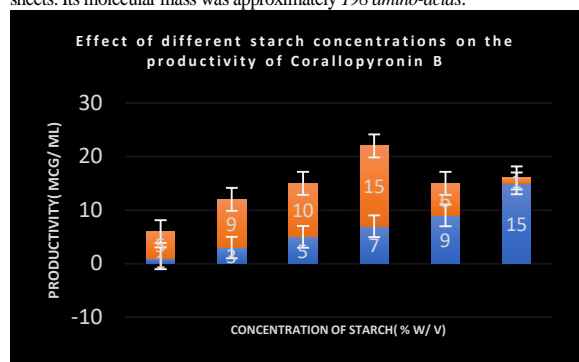


Figure (4). It shows the impact of various concentrations of Soluble starch on the production of *Corallopyronin B*.

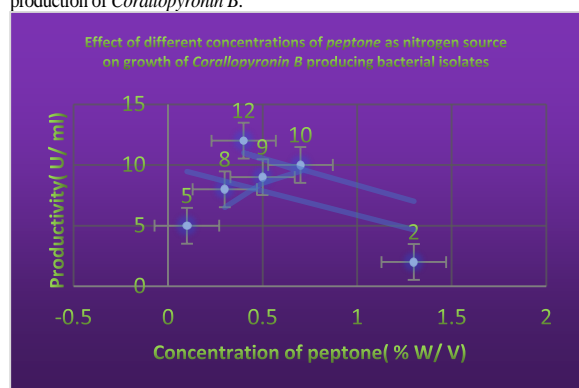


Figure (5). It shows the effects of different Peptone concentrations as nitrogen growth factor on the productivity of *Corallopyronin B*.

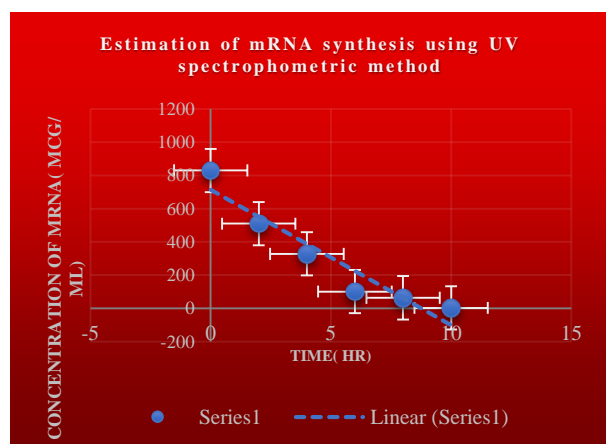


Figure (6). It refers to the estimation of effect of *Corallopyronin B* on microbial mRNA productivity. mRNA synthesis was detected to be diminished proportionately up on employment of exploding doses of *Myxopyronin B* antibiotic.

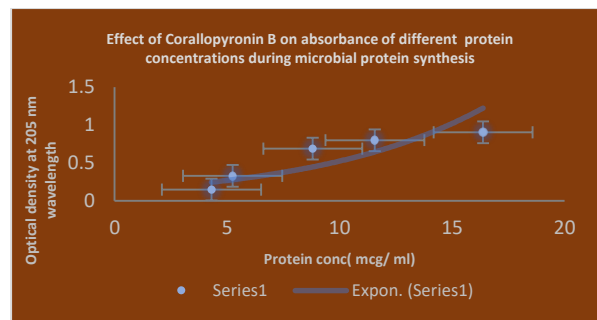


Figure (7). It demonstrates the influence of *Corallopyronin B* on protein synthesis using UV spectrophotometer absorption at 205 nm. Protein synthesis was noticed to be decreased dramatically up on utilization of increasing doses of *Corallopyronin B* antibiotic.

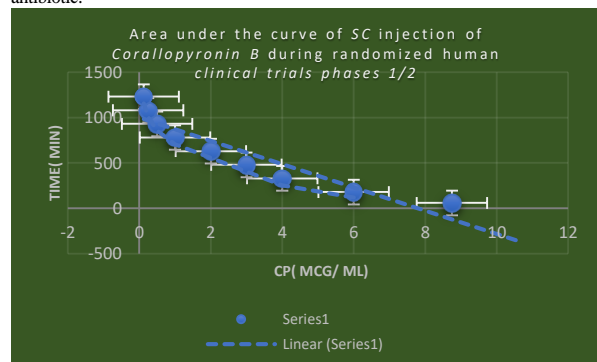


Figure (8). It shows AUC of *Corallopyronin B* following SC administration in randomized human clinical trials stages 1/2. Efficacious dose ranged from 8-9 mg/kg of body weight. Onset of action was observed following closely 15 minutes. It followed first order of elimination kinetics. Bioavailability approximately reached 96%.

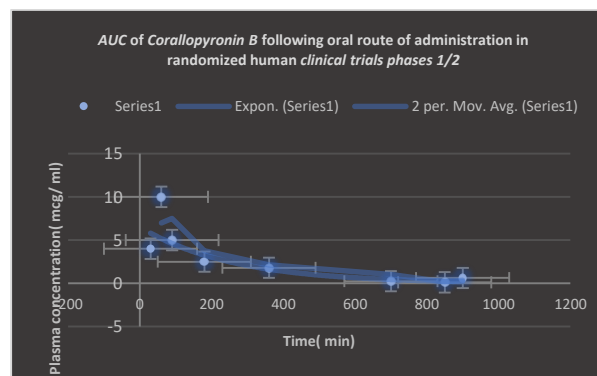


Figure (9). Area under the curve (AUC) following oral administration of *Corallopyronin B* during clinical trials phases 1/2. Efficacious dose ranged from 9.5-10 mg/kg of body weight. Onset of action was observed following nearly 30 minutes. It followed first order of elimination kinetics. Bioavailability reached approximately 95%.

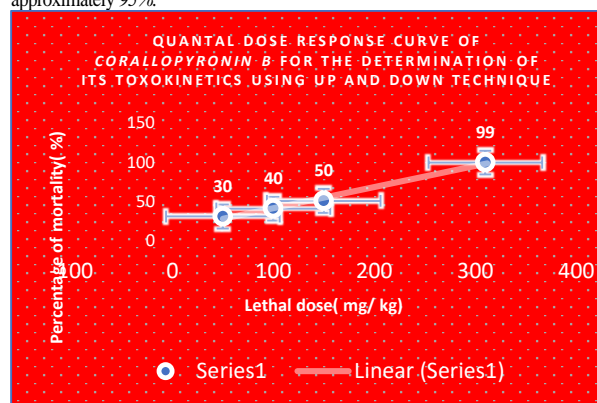


Figure (10). Quantal dose response curve for the determination of toxokinetics of *Corallopyronin B*. LD₅₀ % was found to be 150 mg/kg; while LD₉₉ % was nearly 310 mg/kg.

Statistical analysis: All cultures were conducted in triplets. Their presentation was by means and standard deviation. One way analysis of variance ($p \text{ value} \leq 0.05$) was used as means for performing statistical analysis and also, statistical analysis was based on excel-spreadsheet-software. The *F statistical analysis test* was utilized during the present study.

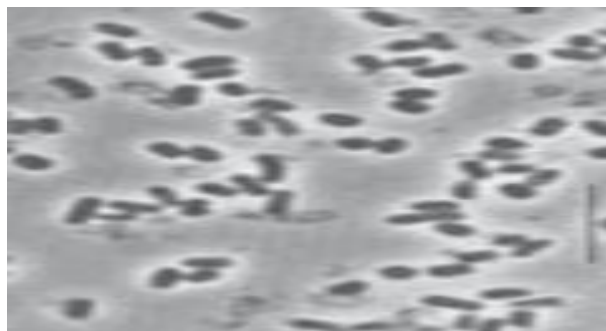


Figure (11). It demonstrates the major *Gram negative* bacterial isolates producing *Corallopyronin B* antibiotic using *Stereomicroscope*.

RESULTS

From the culture supernatant of the soil bacterial isolate *Coralloccoccus coralloides* DSM 2259, which was cultivated on Casein yeast peptone (CYP) plate, *Corallopyronin B* was generated. The test antibiotic prevented the growth of various *Gram +ve* bacteria (MICs ranging from 1 to 10 mcg/ml) and reduced the development of many *Gram -ve* bacteria (including *Escherichia coli*) at MICs more than 100 mcg/ml. Conversely, eukaryotic cells—such as those found in fungi and humans—were unaffected. By preventing bacterial *DNA-dependent RNA polymerase*, the test antibiotic was demonstrated to have a bactericidal effect (RNLP). When 600 mg of the dose per

70 kg of body weight was given SC in phases 1/2 of randomized human clinical trials, the C_{max} was 8.6 mcg/ml at T_{max} of one hour; $T_{1/2}$ reached 136 mins as a result of first order kinetics of elimination. About six to seven hours after SC was given, it ceased working. Less than 6% of experimental candidates experienced unusual toxicity in phases 1/2 of the preclinical and randomized human clinical trials, manifested as decreased bile flow. A detectable 83% protein binding with plasma albumin was found. After the test antibiotics were refined and purified using the reverse phase HPLC technology, *Corallopyronin B* was the predominant component (Table 4).

The 3T3 neutral red uptake phototoxicity test was used to determine the phototoxicity, and it revealed no phototoxicity. However, the Ames test was used to determine the mutagenicity and carcinogenicity of the test antibiotic, and the results showed that there was absolutely no genotoxicity or carcinogenicity. The main isolates of *Gram-negative* bacteria that produce the antibiotic *Corallopyronin B* are shown using a stereomicroscope in Figure 11.

Table (3). It shows the distribution of *Corallopyronin B* producing bacterial isolates

No of +ve bacterial isolates producing <i>Corallopyronin A</i>	No of -ve bacterial isolates producing <i>Corallopyronin A</i>
61	39

Table (4). It demonstrates the degree of purity of test antibiotics following the purification via reversed phase HPLC technique

Test antibiotic	Degree of purity (%)
<i>Corallopyronin A</i>	7
<i>Corallopyronin B</i>	90
<i>Corallopyronin C</i>	3

Table (5). It demonstrates 16 S rRNA detection of *Corallopyronin B* producing isolates using BLASTn software

Description	Query Cover	E value	Per. ident	Acc. Len
<i>Coralloccoccus coralloides</i> DSM 2259, complete genome	100%	0	100	10080619
<i>Coralloccoccus</i> sp. NCCR chromosome, complete genome	100%	0	99.05	9787125
<i>Coralloccoccus coralloides</i> strain B035 chromosome, complete genome	100%	0	98.57	9587888
<i>Coralloccoccus</i> sp. EGB chromosome, complete genome	100%	0	96.83	9431171
<i>Myxococcus fulvus</i> 124B02, complete genome	100%	0	92.08	11048835
<i>Myxococcus</i> sp. MH1 DNA, complete genome	100%	0	91.92	10778154
<i>Myxococcus</i> sp. SDU36 chromosome, complete genome	100%	0	91.63	9016985
<i>Myxococcus xanthus</i> strain GH3.5.6c2 chromosome, complete genome	100%	0	91.28	9321034
<i>Vulgatibacter incomptus</i> strain DSM 27710, complete genome	99%	2.00E-153	82.99	4350553
<i>Anaeromyxobacter</i> sp. Fw109-5, complete genome	99%	1.00E-125	80.43	5277990
Uncultured bacterium clone F5K2Q4C04IF4QS 23S ribosomal RNA gene, partial sequence	77%	3.00E-122	83.53	492
Uncultured bacterium clone F5K2Q4C04I5GUV 23S ribosomal RNA gene, partial sequence	77%	6.00E-114	82.73	491

Table (6). It shows the estimation of zones of inhibition and minimum inhibitory concentrations of Corallopyronin B via Agar diffusion assay using paper discs

Test organism ¹	MIC($\mu\text{g/ml}$)	Diameter of inhibition zone(mm)
<i>Bacillus subtilis</i>	5	10
<i>Staphylococcus aureus</i>	6	16
<i>Streptococcus pneumoniae</i>	10	7
<i>Escherichia coli</i>	119	13
<i>Pseudomonas aeruginosa</i>	129	0
<i>Candida albicans</i>	114	0
<i>Sacchromyces cerevisiae</i>	109	0
<i>Salmonella typhimurium</i>	137	15
<i>Bacillus cereus</i>	14	12
<i>Micrococcus luteus</i>	18	7
<i>Serratia Marcescens</i>	140	10
<i>Mucor hiemalis</i>	0	19
<i>Shigella dysentery</i>	109	14
<i>Proteus mirabilis</i>	123	8
<i>Rickettsiae prowazaki</i>	146	11
<i>Chlamydiae pneumoniae</i>	125	19
<i>Legionella pneumophilla</i>	116	9

Table (7). It demonstrates MICs of Corallopyronin B on different microorganisms using broth microdilution technique

Pathogenic m.o	MIC($\mu\text{g/ml}$)
<i>Bacillus subtilis</i>	10
<i>Bacillus cereus</i>	7
<i>Staphylococcus aureus</i>	9
<i>Pneumococci</i>	6
<i>E.coli</i>	127
<i>Pseudomonas aeruginosa</i>	0
<i>Candida albicans</i>	0
<i>Sacchromyces cerevisiae</i>	0
<i>Salmonella typhimurium</i>	109
<i>Haemophilus influenza</i>	0
<i>Gonococci</i>	105
<i>meningococci</i>	134
<i>Serratia Marcescens</i>	129
<i>Mucor hiemalis</i>	0
<i>Shigella dysenteriae</i>	111
<i>Micrococcus luteus</i>	0
<i>Proteus mirabilis</i>	0
<i>Rickettsiae prowazaki</i>	139
<i>Chlamydiae pneumoniae</i>	131
<i>Legionella pneumophilla</i>	146

Table (8). It demonstrates Minimum bactericidal concentrations(MBCs) of Corallopyronin B on different microorganisms using Broth microdilution technique

Pathogenic m.o	MBC($\mu\text{g/ml}$)
<i>Bacillus subtilis</i>	24
<i>Bacillus cereus</i>	23
<i>Staphylococcus aureus</i>	39
<i>Pneumococci</i>	44
<i>E.coli</i>	338
<i>Pseudomonas aeruginosa</i>	399
<i>Candida albicans</i>	0
<i>Sacchromyces cerevisiae</i>	0
<i>Salmonella typhimurium</i>	320
<i>Haemophilus influenza</i>	0

¹ The initial density of each organism during Agar diffusion assay for the determination of minimum inhibitory concentrations and zones of inhibition of growth was nearly $10^5/\text{ml}$.

Pathogenic m.o	MBC ($\mu\text{g/ml}$)
<i>Gonococci</i>	380
<i>meningococci</i>	377
<i>Serratia Marcescens</i>	307
<i>Mucor hiemalis</i>	0
<i>Shigella dysenteriae</i>	309
<i>Micrococcus luteus</i>	0
<i>Proteus mirabilis</i>	0
<i>Rickettsiae prowazaki</i>	400
<i>Chlamydiae pneumoniae</i>	416
<i>Legionella pneumophilla</i>	252

Table (9). It shows the estimation of mRNA quantity via UV spectrophotometer at 260 nm after addition of Coralopyronin B

mRNA concentration(ng/ ml)	Absorbance(optical density) at 260 nm
600	0.729
567	0.501
204	0.247
25	0.093

Table (10). It shows the effect of Coralopyronin A on the microbial protein synthesis using UV spectrophotometer at 205 nm

Bacterial protein concentration(mcg/ ml)	Time(hr)
91.3	2
45.96	4
28.38	7
3.37	10
0.26	3

Table (11). The resolution of biochemical reactions

Test	Result
Gram stain	-ve rods
Cell shape	Elongated bacilli with tapered ends
Spore shape	Ellipsoidal
Spore site	Central
Motility	+ via gliding
Catalase	+
Oxidase	-
Blood haemolysis	-
Indol	-
Methyl red	-
Nitrate reduction test	+
Voges proscauer	-
Citrate utilization	-
Starch hydrolysis	+
Casein hydrolysis	+
Growth at 45 °C	Bacterial isolates did not grow at 45 °C; but were grown at 10-37 °C
Tween 80	+
Tolerance salinity	
5% NaCl	-
7% NaCl	-
Saccharide fermentation	
Glucose	-
Fructose	-
Maltose	-
Sucrose	-

Tables 10 and 9, respectively, show that there was a considerable decrease in protein synthesis and mRNA synthesis as the dosage of Myxopyronin B was increased. Docking experiments with the MCULE and SWISS DOCK softwares showed that the test antibiotic's mechanism of action was most likely caused by inhibiting RNA

polymerase by binding to its switch region. The test antibiotic's high ΔG was found to be roughly 15 J/mol using the SWISS MODEL software. However, utilizing SWISS MODEL software, it was discovered that the test antibiotic's low K_d near the switch area was roughly -720 nM.

Table 11 provides a summary of the biochemical profile

and morphology of the strong bacterial isolates used in this investigation to produce the test antibiotic.

Corallococcus coralloides DSM 2259 was the most common bacterial isolate that secreted the extracellular test antibiotic, according to its appearance and biochemical responses. The study involved 150 human volunteers in total, with a mean age of 28.9 [8.1] years (SD). The 88% confidence intervals (CIs) for the long transformed ratios of C_{max} , $AUC (0-26)$, and $AUC (0-\infty)$ for the test antibiotic were, in order, 93.3 to 94.6, 90.5 to 95.2, and 90.7 to 93.1. *Corallopyronin B* was found to have a mean protein binding (PB) of about 83%. It was shown that *Albumin* exhibited the predominant protein binding for both Rifampicin and *Corallopyronin B*. The therapeutic activity was discovered to be attributed to the unbound fraction. The structure of *Corallopyronin B*, which was isolated from bacterial isolates of *Corallococcus coralloides* DSM 2259 collected from various soil conditions in Egypt, is depicted in Figure 1.

Using a mass spectrometer, the molecular formula of the purified test antibiotic was found to be $C_{31}H_{43}NO_7$. The area under the curve (AUC) after oral *Corallopyronin B* dosing during phases 1/2 of clinical trials is shown in Figure 9. The range of effective doses was 9.5–10 mg/kg of body weight. The action started after over thirty minutes. It adhered to the kinetics of first order elimination. The quantal dosage response curve for the assessment of *Corallopyronin B*'s toxicokinetics is displayed in Figure 10. It was discovered that $LD_{50}\%$ was 150 mg/kg and $LD_{99}\%$ was around 310 mg/kg. The AUC of *Corallopyronin B* after SC injection in phases 1/2 of randomized human clinical trials is displayed in Figure 8.

The range of effective doses was 8–9 mg/kg of body weight. The beginning of the action was noted after a close 15 minutes. It adhered to the kinetics of first order elimination. The docking of the *Corallopyronin B* ligand on Bacterial RNA polymerase is shown in Figure 2. High affinity and an inhibitory impact were demonstrated by *Corallopyronin B* towards the RNA polymerase switch region. Figure 7 uses the UV spectrophotometer absorbance at 205 nm to illustrate how *Corallopyronin B* affects protein synthesis. A significant reduction in protein synthesis was seen upon administration of escalating dosages of the antibiotic *Corallopyronin B*. The three-dimensional structure of bacterial prokaryotic RNA polymerase is depicted in Figure 3.

This structure includes the switch binding site, to which *Corallopyronin B* Ligand binds strongly, inhibiting the activity of bacterial RNA polymerase selectively, which in

turn causes the inhibition of mRNA transcription and ultimately the death of the microbe. Alpha and Beta spiral sheets made up the RNA polymerase enzyme's secondary structure. It had a molecular mass of about 198 amino acids. Figure 6 speaks about estimating Corallopyronin B's impact on the productivity of microbial mRNA. An increase in the dosage of the antibiotic *Myxopyronin B* was found to cause a commensurate decrease in mRNA production. The effects of varying peptone concentrations as a nitrogen growth factor on *Corallopyronin B* production are depicted in Figure 5.

The effect of different soluble starch concentrations on the synthesis of *Corallopyronin B* is depicted in Figure 4. The resolution of biological reactions is shown in Table 11. Table 8 uses the Broth microdilution technique to show the minimum bactericidal concentrations (MBCs) of *Corallopyronin B* on various bacteria. The measurement of the amount of mRNA using a UV spectrophotometer at 260 nm following the addition of *Corallopyronin B* is displayed in Table 9. The distribution of bacterial isolates that produce *Corallopyronin B* is displayed in Table 3. The degree of purity of the test antibiotics after they were purified using the reversed phase HPLC process is shown in Table 4.

Table 5 shows how to use BLASTn software to detect 16S rRNA in isolates that produce *Corallopyronin B*. Table 7 shows *Corallopyronin B*'s minimum inhibitory concentrations (MICs) on several bacteria using the broth microdilution method. *Corallopyronin B*'s zones of inhibition and minimum inhibitory concentrations are estimated using the Agar diffusion assay with paper discs, as shown in Table 6.

DISCUSSION

Globally, exploding morbidity and mortality due to antibiotic-resistant micro-organism infections was observed. Hence, amended hindrance and touchstone of infectious diseases, as well as appropriate use of approved antibacterial drugs were essential. The in vitro and in vivo antimicrobial activity of *Corallopyronin B*, a novel antibiotic was evaluated in the present study. It demonstrated excellent bactericidal activity against a broad spectrum of *G +ve* bacteria with MICs did not exceed 20 mcg/ml. On the other hand, it showed broad bactericidal activities against *G -ve* bacteria with minimal inhibitory concentrations were greater than 100 mcg/ml. Its mechanism of action was realized during the investigation of RNA synthesis to be via the inhibition of prokaryotic DNA-dependent-RNA polymerase; whereas no inhibitory impact was observed for Eukaryotic one. Docking studies through SWISS DOCK software confirmed this as well. The

antibiotic activities *Corallopyronin A, B* and *C* were isolated from the culture supernatant of 29 bacterial isolates of *Myxobacterium Corallococcus coralloides* DSM 2259 detected molecularly using *16 S rRNA* technique (table 3).

The antibiotic activity did not inhibit the growth or kill eukaryotic cells such as human and fungal cells reflecting selectivity towards the inhibition of the growth of prokaryotic bacterial cells. This selectivity effect minimized the adverse effects noticed during the present study. Docking studies via *SWISS DOCK* software revealed that desmethylation of either *Corallopyronin A, B, C* enhanced its biological activity. Purification was performed through reversed phase *HPLC*. *Corallopyronin B* was the main refined antibiotic. Its purity degree reached approximately 90 %; while, the remaining purified antibiotics were detected to be *Corallopyronin A* (7%) and *C* (3%). The antibacterial activity was assessed via the determination of *MICs* of the test antibiotics using the agar diffusion technique utilizing paper discs 5 mm in diameter and the broth dilution assay. The initial density of each test microorganism was about $10^5/ml$ of the culture suspension. The *MICs* of test antibiotic against *G +ve* bacteria ranged from 6 to 20 mcg/ml; Whereas *MICs* reached above 100 mcg/ml against some selected *G -ve* bacteria. On the other hand no effect was detected against the growth of fungi and yeasts. **Irschik H et al.** stated that *Myxovalargin A* was a novel peptide antibiotic isolated from the culture supernatant of the *myxobacterium Myxococcus fulvus* strain *Mx f65*. It was active against *Gram-positive* bacteria (*MIC* 0.3 approximately 5 micrograms/ml), at higher concentrations also against *Gram-negative* ones (*MIC* 6 approximately 100 micrograms/ml), and not at all against yeasts and molds. Its mechanism of action involved the inhibition of the bacterial protein synthesis⁽⁵⁰⁾.

According to **Glaus F et al.**, *Ripostatin*, a novel antibiotic, isolated from the culture supernatant of *Myxobacterium, Sorangium cellulosum* strain *so ce377*. On the other hand it interfered of the bacterial *RNA* synthesis⁽⁵¹⁾.

On the other hand, *Corallopyronin B* was found to be structurally related to α -pyrone antibiotics from *myxobacteria*. Its ability to inhibit *RNA polymerase* was through interaction with the switch region of *RNA polymerase*; while *Rifampicin* inhibited the same enzyme through different region⁽⁵²⁾.

Myxopyronin showed no phototoxicity and mutagenicity in rabbit animal models during the *preclinical trials stage*, in the present study. Rare adverse effects including cholestatic jaundice were reported in less than 5% of the experimental subjects received the test antibiotics during

randomized human clinical trials phases 1/2. The biological half-life of *Corallopyronin B* reached approximately 2.25 hours. 0.4 % *peptone* and 7 % *soluble starch* were detected to be the optimal nitrogen and carbon growth factors for bacterial isolates producing the test antibiotics, respectively (figures 4 and 5).

High ΔG of the test antibiotic was observed to be approximately 15 J/ mole as determined via *SWISS MODEL* software reflecting high catalytic activity of the test antibiotic towards the switch region. On the other hand, low *Kd* of the test antibiotic towards the switch region was found to be approximately -720 nM using *SWISS MODEL* software indicating high affinity and binding capacity. Bioavailability studies were performed using *HPLC* during randomized human clinical trials phases 1/2 revealed that *Corallopyronin B* reached nearly 95% oral bioavailability, 96% IM bioavailability and 100% IV bioavailability.

Metabolic studies using *HPLC* revealed that the test antibiotic showed no in vivo induction of hepatic metabolizing *Cytochrome P450* enzymatic system; while *Rifampicin* induced *CYP3A4* hepatic metabolizing enzyme potently. Up and down procedure intended for the evaluation of acute toxicity profile of the test antibiotic showed that *LD₅₀* was about 150 mg/kg body weight; while *LD₉₉* reached 310 mg/kg. On the other hand, therapeutic margin of the test antibiotic ranged from 7 mcg/ml to 100 mcg/ml. *Corallopyronin B* producing bacterial isolates were gram negative, spore forming *obligate aerobes* and *chemoorganotrophic*. They were *elongated rods with tapered ends*. No *flagella* were present; but the cells moved via *gliding*. They fermented *Tween 80, starch* and *casein*. On the other hand they were positive for *catalase* while negative for *oxidase* tests. They reduced *nitrates*

And were able to grow at 10-37 °C. A total of 150 human subjects (mean *SD* age, 27.3 [8.6] years) were enrolled and completed the study. The 88% confidence intervals (CIs) for the long transformed ratios of *C_{max}*, *AUC* (0-26), and *AUC* (0- ∞) for the test antibiotic were, in order, 93.3 to 94.6, 90.5 to 95.2, and 90.7 to 93.1, respectively. The point estimates for *C_{max}* in the present study were outside the limit for bio-equivalence for *Rifampicin* standard drug. The mean *PB* was observed for *Corallopyronin B* which approximated 83% while that of *Rifampicin* reached 88%⁽⁵³⁾.

It was noticed that plasma protein binding was proportionally increased with increasing the doses of the test antibiotic. The plasma protein binding participated in extending the *Corallopyronin B* duration of action. The

major protein binding for *Corallopyronin B* and *Rifampicin* was noticed to be *Albumin*. The unbound fraction was detected to be responsible for the therapeutic activity.

Conclusion: Antibiotic resistance is a global challenge that the current study shows promise in solving. According to the findings of the current study, *Corallopyronin B*, which was isolated from the bacterial isolates *Corallococcus coralloides* DSM 2259 that were collected from various soil environments in Egypt, exhibited significant antibiotic activity both in vitro and in vivo against a moderate range of pathogenic bacteria, particularly *G+ve* varieties. Future research is recommended to investigate pharmacological interactions of the synergism type between *Corallopyronin A* and different antibiotic classes.

DECLARATIONS

Funding:

This study was funded by the single author.

Conflict of interest/ Competing of interests:

There is no conflict of interest; as well as no competing of interests exist.

Ethics approval and consent to participate:

All informed consent from all participants in the present study was obtained. All relevant institutional, national, and/or worldwide standards pertaining to the use and care of humans and animals were given priority in the current study. The Ethical Committee for Human and Animal Handling at Cairo University (*ECAHCU*), housed at the Faculty of Pharmacy, Cairo University, Egypt, approved all study procedures involving humans and animals in accordance with the recommendations of the Weatherall Report (approval number *T716/2022*). The number and degree of suffering of the study's human and animal participants were minimized at all costs. The randomized human clinical trials registration number *NXT00000381* was authorized by *EMA* in Egypt. Date of registration was *7 June 2023*.

Data availability and material:

Data and material used are deposited in GenBank with accession numbers: *PQ049657* and *PQ049658*.

Acknowledgement:

Not applicable

REFERENCES

1. Dalhoff A. Selective toxicity of antibacterial agents-still a valid concept or do we miss chances and ignore risks? *Infection*. 2021 Feb; 49(1):29-56. doi: 10.1007/s15010-020-01536-y.
2. Hutchings MI, Truman AW, Wilkinson B. Antibiotics: past, present and future. *Curr Opin Microbiol*. 2019 Oct; 51:72-80. doi: 10.1016/j.mib.2019.10.008.
3. Wenciewicz TA. Crossroads of Antibiotic Resistance and Biosynthesis. *J Mol Biol*. 2019;431(18):3370-3399. doi: 10.1016/j.jmb.2019.06.033.
4. Lepe JA, Martínez-Martínez L. Resistance mechanisms in Gram-negative bacteria. *Med Intensiva (Engl Ed)*. 2022 Jul;46(7):392-402. doi: 10.1016/j.medine.2022.05.004.
5. Vila J, Marco F. [Interpretive reading of the non-fermenting gram-negative bacilli antibiogram]. *Enferm Infecc Microbiol Clin*. 2010 Dec;28(10):726-36. Spanish. doi: 10.1016/j.eimc.2010.05.001.
6. Mushtaq S, Vickers A, Woodford N, Livermore DM. WCK 4234, a novel diazabicyclooctane potentiating carbapenems against Enterobacteriaceae, Pseudomonas and Acinetobacter with class A, C and D β -lactamases. *J Antimicrob Chemother*. 2017 Jun 1; 72(6):1688-1695. doi: 10.1093/jac/dkx035.
7. Irwin SV, Fisher P, Graham E, Malek A. Sulfites inhibit the growth of four species of beneficial gut bacteria at concentrations regarded as safe for food. *PLoS One*. 2017; 12 (10): e0186629. doi: 10.1371/ journal.pone.0186629.
8. Jeong S, Lee Y, Yun CH, Park OJ, Han SH. Propionate, together with triple antibiotics, inhibits the growth of Enterococci. *J Microbiol*. 2019 Nov; 57(11):1019-1024. doi: 10.1007/s12275-019-9434-7.
9. Kohanski MA, Dwyer DJ, Hayete B, Lawrence CA, Collins JJ. A common mechanism of cellular death induced by bactericidal antibiotics. *Cell*. 2007 Sep 7;130(5):797-810. doi: 10.1016/j.cell.2007.06.049.
10. Brauer M, Herrmann J, Zühlke D, Müller R, Riedel K, Sievers S. Myxopyronin B inhibits growth of a Fidaxomicin-resistant *Clostridioides difficile* isolate and interferes with toxin synthesis. *Gut Pathog*. 2022 Jan 6; 14(1):4. doi: 10.1186/s13099-021-00475-9.
11. Doundoulakis T, Xiang AX, Lira R, Agrios KA, Webber SE, Sisson W, et al. Myxopyronin B analogs as inhibitors of RNA polymerase, synthesis and biological evaluation. *Bioorg Med Chem Lett*. 2004 Nov 15; 14(22):5667-72. doi: 10.1016/j.bmcl.2004.08.045.
12. Lira R, Xiang AX, Doundoulakis T, Biller WT, Agrios KA, Simonsen KB, et al. Syntheses of novel myxopyronin B analogs as potential inhibitors of bacterial RNA polymerase. *Bioorg Med Chem Lett*. 2007 Dec 15; 17 (24): 6797-800. doi: 10.1016/j.bmcl.2007.10.017.

13. Moy TI, Daniel A, Hardy C, Jackson A, Rehrauer O, Hwang YS, et al. Evaluating the activity of the RNA polymerase inhibitor myxopyronin B against *Staphylococcus aureus*. *FEMS Microbiol Lett*. 2011 Jun;319(2):176-9. doi: 10.1111/j.1574-6968.2011.02282.x.
14. Srivastava A, Talaue M, Liu S, Degen D, Ebricht RY, Sineva E, et al. New target for inhibition of bacterial RNA polymerase: 'switch region'. *Curr Opin Microbiol*. 2011 Oct; 14(5):532-43. doi: 10.1016/j.mib.2011.07.030.
15. Mosaei H, Harbottle J. Mechanisms of antibiotics inhibiting bacterial RNA polymerase. *Biochem Soc Trans*. 2019 Feb 28; 47(1):339-350. doi: 10.1042/BST20180499.
16. Sucipto H, Sahner JH, Prusov E, Wenzel SC, Hartmann RW, Koehnke J, Müller R. In vitro reconstitution of α -pyrone ring formation in myxopyronin biosynthesis. *Chem Sci*. 2015 Aug 1;6(8):5076-5085. doi: 10.1039/c5sc01013f.
17. O'Toole GA. Classic Spotlight: How the Gram Stain Works. *J Bacteriol*. 2016; 198 (23): 3128. doi:10.1128/JB.00726-16.
18. Luhur J, Chan H, Kachappilly B, Mohamed A, Morlot C, Awad M, et al. A dynamic, ring-forming MucB / RseB-like protein influences spore shape in *Bacillus subtilis*. *PLoS Genet*. 2020 Dec 14;16(12):e1009246. doi: 10.1371/journal.pgen.1009246.
19. Qin Y, Faheem A, Hu Y. A spore-based portable kit for on-site detection of fluoride ions. *J Hazard Mater*. 2021 Oct 5; 419:126467. doi: 10.1016/j.jhazmat.2021.126467.
20. Cabeen MT, Jacobs-Wagner C. Bacterial cell shape. *Nat Rev Microbiol*. 2005;3(8):601-10. doi: 10.1038/nrmicro1205.
21. Wang Q, Xiao L, He Q, Liu S, Zhang J, et al. Comparison of haemolytic activity of tentacle-only extract from jellyfish *Cyanea capillata* in diluted whole blood and erythrocyte suspension: diluted whole blood is a valid test system for haemolysis study. *Exp Toxicol Pathol*. 2012 Nov;64(7-8):831-5. doi: 10.1016/j.etp.2011.03.003.
22. Dubay MM, Acres J, Riekeles M, Nadeau JL. Recent advances in experimental design and data analysis to characterize prokaryotic motility. *J Microbiol Methods*. 2023; 204:106658. doi: 10.1016/j.mimet.2022.106658.
23. Wang C, Zhang Y, Luo H, Zhang H, Li W, Zhang WX, Yang J. Iron-Based Nanocatalysts for Electrochemical Nitrate Reduction. *Small Methods*. 2022 Oct;6(10):e2200790. doi: 10.1002/smt.202200790.
24. Hu CY, Cheng HY, Yao XM, Li LZ, Liu HW, Guo WQ, Fu JL. Biodegradation and decolourization of methyl red by *Aspergillus versicolor* LH1. *Prep Biochem Biotechnol*. 2021; 51 (7): 642-649. doi: 10.1080/ 10826068.2020. 1848868.
25. Xu D, Wu L, Yao H, Zhao L. Catalase-Like Nanozymes: Classification, Catalytic Mechanisms, and Their Applications. *Small*. 2022 Sep; 18 (37):e2203400. doi: 10.1002/sml.202203400.
26. Pawlik A, Stefanek S, Janusz G. Properties, Physiological Functions and Involvement of Basidiomycetous Alcohol Oxidase in Wood Degradation. *Int J Mol Sci*. 2022 Nov 9;23 (22):13808. doi: 10.3390/ijms232213808.
27. Cordaro JT, Sellers W. Blood coagulation test for citrate utilization. *Appl Microbiol*. 1968 Jan;16(1):168-9. doi: 10.1128/am.16.1.168-169.1968.
28. Krajang M, Malairuang K, Sukna J, Rattanapradit K, Chamsart S. Single-step ethanol production from raw cassava starch using a combination of raw starch hydrolysis and fermentation, scale-up from 5-L laboratory and 200-L pilot plant to 3000-L industrial fermenters. *Biotechnol Biofuels*. 2021;14:68. doi:10.1186/s13068-021-01903-3.
29. Kerwin BA. Polysorbates 20 and 80 used in the formulation of protein biotherapeutics: structure and degradation pathways. *J Pharm Sci*. 2008 Aug;97(8):2924-35. doi: 10.1002/jps.21190.
30. Trueba FJ, Neijssel OM, Woldringh CL. Generality of the growth kinetics of the average individual cell in different bacterial populations. *J Bacteriol*. 1982 Jun; 150(3):1048-55. doi: 10.1128/jb.150.3.1048-1055.1982.
31. McCrea KW, Xie J, LaCross N, Patel M, Mukundan D, Murphy TF. Relationships of non-typeable *Haemophilus influenzae* strains to hemolytic and nonhemolytic *Haemophilus haemolyticus* strains. *J Clin Microbiol*. 2008; 46 (2): 406-16. doi: 10.1128/JCM.01832-07.
32. Jogawat A, Vadassery J, Verma N, Oelmüller R, Dua M, Nevo E, Johri AK. PiHOG1, a stress regulator MAP kinase from the root endophyte fungus *Piriformospora indica*, confers salinity stress tolerance in rice plants. *Sci Rep*. 2016 Nov 16; 6:36765. doi: 10.1038/srep36765.
33. Barry AL, Feeney KL. Two quick methods for Voges-Proskauer test. *Appl Microbiol*. 1967 Sep;15(5):1138-41. doi: 10.1128/am.15.5.1138-1141.1967.
34. Wang J, Su Y, Jia F, Jin H. Characterization of casein hydrolysates derived from enzymatic hydrolysis. *Chem Cent J*. 2013;7(1):62. doi: 10.1186/1752-153X-7-62.
35. de Bie TH, Witkamp RF, Balvers MG, Jongsma MA. Effects of γ -aminobutyric acid supplementation on glucose control in adults with prediabetes: A double-blind, randomized, placebo-controlled trial. *Am J Clin Nutr*. 2023;118(3):708-719. doi: 10.1016/j.ajcnut.2023.07.017.

36. Endoh R, Horiyama M, Ohkuma M. D-Fructose Assimilation and Fermentation by Yeasts Belonging to *Saccharomycetes*: Rediscovery of Universal Phenotypes and Elucidation of Fructophilic Behaviors in *Ambrosiozyma platypodis* and *Cyberlindnera americana*. *Micro-organisms*. 2021;9(4):758. doi: 10.3390/microorganisms9040758.
37. Lu Z, Guo W, Liu C. Isolation, identification and characterization of novel *Bacillus subtilis*. *J Vet Med Sci*. 2018 Mar 24;80(3):427-433. doi: 10.1292/jvms.16-0572.
38. Zhao Y, Meng K, Fu J, Xu S, Cai G, Meng G, Nielsen J, Liu Z, Zhang Y. Protein engineering of invertase for enhancing yeast dough fermentation under high-sucrose conditions. *Folia Microbiol (Praha)*. 2023 Apr;68(2):207-217. doi: 10.1007/s12223-022-01006-y.
39. Irschik H, Gerth K, Höfle G, Kohl W, Reichenbach H. The *myxopyronins*, new inhibitors of bacterial RNA synthesis from *Myxococcus fulvus* (*Myxobacterales*). *J Antibiot (Tokyo)*. 1983 Dec; 36 (12): 1651-8. doi: 10.7164/antibiotics.36.1651.
40. Wiegand I, Hilpert K, Hancock RE. Agar and broth dilution methods to determine the minimal inhibitory concentration (MIC) of antimicrobial substances. *Nat Protoc*. 2008;3(2):163-75. doi: 10.1038/nprot.2007.521.
41. Balouiri M, Sadiki M, Ibensouda SK. Methods for in vitro evaluating antimicrobial activity: A review. *J Pharm Anal*. 2016;6(2):71-79. doi: 10.1016/j.jpha.2015.11.005.
42. Dell'Anno A, Fabiano M, Duineveld GCA, Kok A, Danovaro R. Nucleic acid (DNA, RNA) quantification and RNA/DNA ratio determination in marine sediments: comparison of spectrophotometric, fluorometric, and High Performance liquid chromatography methods and estimation of detrital DNA. *Appl Environ Microbiol*. 1998 Sep;64(9):3238-45. doi: 10.1128/AEM.64.9.3238-3245.1998.
43. Simonian MH. Spectrophotometric determination of protein concentration. *Curr Protoc Cell Biol*. 2002 Aug; Appendix 3: Appendix 3B. doi: 10.1002/0471143030.cba03bs15.
44. Rox K, Becker T, Schiefer A, Grosse M, Ehrens A, Jansen R, et al. Pharmacokinetics and Pharmacodynamics (PK/PD) of Coralopyronin A against Methicillin-Resistant *Staphylococcus aureus*. *Pharmaceutics*. 2022 Dec 30; 15 (1): 131. doi: 10.3390/pharmaceutics15010131.
45. Xu J, Jin H, Zhu H, Zheng M, Wang B, Liu C, et al. Oral bioavailability of rifampicin, isoniazid, ethambutol, and pyrazinamide in a 4-drug fixed-dose combination compared with the separate formulations in healthy Chinese male volunteers. *Clin Ther*. 2013; 35(2):161-8. doi: 10.1016/j.clinthera.2013.01.003.
46. Utku Türk EG, Jannuzzi AT, Alpertunga B. Determination of the Phototoxicity Potential of Commercially Available Tattoo Inks Using the 3T3-neutral Red Uptake Phototoxicity Test. *Turk J Pharm Sci*. 2022 Feb 28; 19 (1): 70-75. doi: 10.4274/tjps.galenos.2021.86344.
47. Thomas DN, Wills JW, Tracey H, Baldwin SJ, Burman M, Williams AN, Harte DSG, Buckley RA, Lynch AM. Ames Test study designs for nitrosamine mutagenicity testing: qualitative and quantitative analysis of key assay parameters. *Mutagenesis*. 2023 Dec 19;gead033. doi: 10.1093/mutage/gead033.
48. Zhang, YY., Huang, YF., Liang, J. et al. Improved up-and-down procedure for acute toxicity measurement with reliable LD50 verified by typical toxic alkaloids and modified Karber method. *BMC Pharmacol Toxicol* 23, 3 (2022). <https://doi.org/10.1186/s40360-021-00541-7>.
49. Heuser E, Becker K, Idelevich EA. Bactericidal Activity of Sodium Bituminosulfonate against *Staphylococcus aureus*. *Antibiotics (Basel)*. 2022 Jul 5;11(7):896. doi: 10.3390/antibiotics11070896.
50. Irschik H, Gerth K, Kemmer T, Steinmetz H, Reichenbach H. The myxovalargins, new peptide antibiotics from *Myxococcus fulvus* (*Myxobacterales*). I. Cultivation, isolation, and some chemical and biological properties. *J Antibiot (Tokyo)*. 1983 Jan;36(1):6-12. doi: 10.7164/antibiotics.36.6.
51. Glaus F, Dedić D, Tare P, Nagaraja V, Rodrigues L, Aínsa JA, et al. Total Synthesis of Ripostatin B and Structure-Activity Relationship Studies on Ripostatin Analogs. *J Org Chem*. 2018;83(13):7150-7172. doi: 10.1021/acs.joc.8b00193.
52. Dennison TJ, Smith JC, Badhan RKS, Mohammed AR. Formulation and Bioequivalence Testing of Fixed-Dose Combination Orally Disintegrating Tablets for the Treatment of Tuberculosis in the Paediatric Population. *J Pharm Sci*. 2020 Oct;109(10):3105-3113. doi: 10.1016/j.xphs.2020.07.016.
53. Alghamdi WA, Al-Shaer MH, Peloquin CA. Protein Binding of First-Line Antituberculosis Drugs. *Antimicrob Agents Chemother*. 2018 Jun 26;62(7):e00641-18. doi: 10.1128/AAC.00641-18.



E-ISSN: 2833-3772 | Volume 4 (2025), Issue 1 | Jan-Feb 2025

The Scientific Journal of Medical Scholar

Publisher and Owner: Real-Publishers Limited (Realpub LLC)

30 N Gould St Ste R, Sheridan, WY 82801, USA

Associate Publisher: The Scientific Society of Educational Services Development [SSESD], Egypt

Website: <https://realpublishers.us/index.php/sjms/index>